ON ITERATIVE SOURCE-CHANNEL IMAGE DECODING WITH MARKOV RANDOM FIELD SOURCE MODELS

Jörg Kliewer [1], *Norbert Görtz* [2], *and Alfred Mertins* [3]

[1] University of Kiel, Institute for Circuits and Systems Theory (LNS)
24143 Kiel, Germany, jkl@tf.uni-kiel.de

[2] Munich University of Technology (TUM), Institute for Communications Engineering (LNT)
80290 Munich, Germany, norbert.goertz@ei.tum.de

[3] University of Oldenburg, Signal Processing Group
26111 Oldenburg, Germany, alfred.mertins@uni-oldenburg.de

ABSTRACT

In this paper we propose a novel iterative source-channel decoding approach for robust transmission of compressed still images over noisy communication channels. Besides the explicit redundancy introduced by channel encoding also implicit residual source redundancy is exploited for error protection. The source redundancy is modeled by a Markov random field (MRF) source model, which considers the residual spatial correlation after source encoding. The resulting MRF-based soft-input/soft-output source decoder is used as outer constituent decoder in the proposed iterative source-channel decoding scheme, where due to the link between MRFs and the Gibbs distribution, the source decoder can be implemented with very low complexity. We show that this iterative decoding scheme can be successfully employed for recovering the image data, especially when the channel is highly corrupted.

1. INTRODUCTION

Joint source-channel coding approaches for robust image transmission have recently become a reasonable alternative for delay- or complexity-constrained systems compared to the strictly separate design of source and channel encoder. One subclass of those approaches is characterized by a joint allocation of source and channel coding rates in combination with a strong error protection scheme (e.g. [1,2]), which provides excellent results for moderately distorted channels. However, especially for low channel signal-to-noise ratios (SNRs) the performance highly depends on the properties of the used channel codes. Another subclass is represented by joint source-channel decoding where residual source redundancy is exploited for additional error protection at the decoder (e.g. [3, 4]). These methods have less encoding delay and complexity, and for very low channel SNRs, they often yield similar or better performance than the combination of strong source and channel encoding [5].

In this paper, we address joint source-channel decoding and utilize both the implicit residual index correlation after source-encoding and the explicit redundancies from channel codes for protecting the source data. As a new result the two-dimensional residual spatial correlation of the source image is modeled via a Markov random field (MRF) approach [6], which has the advantage that it is not necessary to store a priori information describing the residual source correlation at the decoder. This is in contrast to those approaches which model the image data as Gauss-Markov processes, as for example the methods proposed in [4, 7]. The proposed technique utilizes an iterative source-channel decoding scheme analog to the decoding of serially concatenated channel codes [8], where the outer constituent soft-input/soft-output (SISO) channel decoder is replaced by the MRF-based SISO source decoder.

2. TRANSMISSION SYSTEM

The block diagram of the overall transmission system is depicted in Fig. 1. The two-dimensional (2-D) subband image is scanned

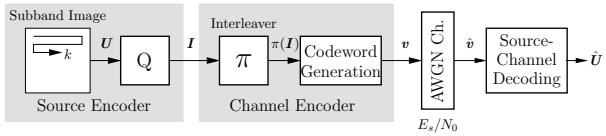

Fig. 1. Model of the transmission system

in order to obtain the one-dimensional (1-D) subband vector $\boldsymbol{U} = [U_0, U_1, \ldots, U_{N-1}]$ consisting of N source values U_k. After subsequent (vector-) quantization, the resulting indices $I_k \in \mathcal{I}$ are represented with M bits where $\mathcal{I} = \{0, 1, \ldots, 2^M - 1\}$. We can generally assume that there are dependencies between the elements of the index vector $\boldsymbol{I} = [I_0, I_1, \ldots, I_{N-1}]$ due to delay and complexity constraints for the source encoder.

After interleaving and channel encoding with a rate-R systematic channel code we obtain the code bit vector $\boldsymbol{v} = [\pi(\boldsymbol{I}), \boldsymbol{c}]$ where $\boldsymbol{v} = [v_0, v_1, \ldots, v_{N_v-1}]$ with $v_k \in \{0, 1\}$, $N_v = N \cdot M/R$, and $\boldsymbol{c}$ referring to the redundancy bits. The code bit vector $\boldsymbol{v}$ is then transmitted over a BPSK-modulated AWGN channel. The conditional p.d.f. for the received soft bit $\hat{v}_m \in \mathbb{R}$ at the channel output given the transmitted bit v_m, $m = 0, 1, \ldots, N_v - 1$, can be written as

$$p(\hat{v}_m \mid v_m) = \frac{1}{\sqrt{2\pi}\sigma_e} \, e^{-\frac{1}{2\sigma_e^2}(\hat{v}_m - v'_m)^2}, \quad v'_m = 1 - 2\, v_m, \quad (1)$$

and $\sigma_e^2 = \frac{N_0}{2E_s}$ denoting the channel noise variance. E_s is the energy to transmit each bit, and N_0 corresponds to the one-sided power spectral density of the noise. Using conditional log-

likelihood ratios (L-values) we may express (1) also as

$$L(\hat{v}_m \mid v_m) = \ln\left(\frac{p(\hat{v}_m \mid v_m = 0)}{p(\hat{v}_m \mid v_m = 1)}\right) = 4\,\frac{E_s}{N_0}\,\hat{v}_m = L_c\,\hat{v}_m. \quad (2)$$

The source-channel decoding step in Fig. 1 then provides an estimate of the input vector $\boldsymbol{U}$ in such a way that the SNR at the decoder output is maximized.

3. MRF-BASED SISO SOURCE DECODING

In this section only the residual source redundancy after source encoding is exploited for error protection, i.e. no channel codes are used. Thus, in the transmission system from Fig. 1 we therefore have $\boldsymbol{v} = \boldsymbol{I}$. For this scenario we derive a SISO source decoder based on a MRF source model which generates a posteriori probabilities (APPs) for the source hypotheses $I_k = \lambda$.

To this end, let us consider the eight nearest neighbors for a given subband source index I_k within a quantized subband image *prior* to transmission. Such a neighborhood system is displayed in Fig. 2(a), where all neighboring source indices are referenced relatively to the index $I_{k,0,0}$ under consideration, which for the sake of brevity will also simply be written as I_k in all future discussions. We denote the set of all source indices belonging to the neighborhood of I_k as $\mathcal{N}_{I_k} = \{I_{k,q,j}\colon\ q,j = -1,0,1\}\backslash I_k$ in the following. Since all indices in the neighborhood system of Fig. 2(a) show spatial dependencies due to imperfect source encoding the index probabilities $P(I_k = \lambda)$, $\lambda \in \mathcal{I}$, may be modeled via a MRF using the well-known Markov-Gibbs correspondence [6]. Using this relation, the probability for an element I_k of the MRF given all other source indices in a local neighborhood $\mathcal{N}_{I_k}$ can then be stated as [6]

$$P(I_k = \lambda \,|\, \mathcal{N}_{I_k}) = \frac{1}{Z}\, e^{-\frac{1}{T}U(\lambda, \mathcal{N}_{I_k})}, \quad (3)$$

where the function $U(\lambda, \mathcal{N}_{I_k})$ is called energy function, the quantity T is called temperature, and Z denotes a normalization constant. We can decompose $U(\lambda, \mathcal{N}_{I_k})$ as a sum over so-called potential functions $V_C(\lambda, \mathcal{N}_{I_k})$ according to

$$U(\lambda, \mathcal{N}_{I_k}) = \sum_C V_C(\lambda, \mathcal{N}_{I_k}). \quad (4)$$

The potential functions are defined for a given clique C, and the sum in (4) is carried out over all or a subset of all possible cliques in the local neighborhood. An example is depicted in Fig. 2(b) for the eight-pixel neighborhood system in Fig. 2(a) where all associated cliques are shown. The first type of clique just consists of single source indices, the second type of cliques describes the index I_k and its horizontal neighbors, the third type addresses all vertical neighbors of I_k and so on. In the following we restrict ourselves only to two-element cliques and the potential functions

$$V_C(\lambda, I_{k,q,j}) = |\lambda - I_{k,q,j}|^{\delta} \quad (5)$$

proposed in [9], where δ is a free parameter.

In order to apply the MRF model to the source decoder we consider a new set $\mathcal{N}_{\tilde{I}_k} = \{\tilde{I}_{k,q,j}\colon\ q,j = -1,0,1\}\backslash\tilde{I}_k$ where $\tilde{I}_{k,q,j}$ now denotes an *already decoded* estimate of $I_{k,q,j}$, e.g. from a maximum-likelihood (ML) decoding of the received soft-bits at the channel output. The APPs for $I_k = \lambda$ based on the local neighborhood at the decoder can then be written as $P(I_k = \lambda \,|\, \hat{I}_k, \mathcal{N}_{\tilde{I}_k})$,

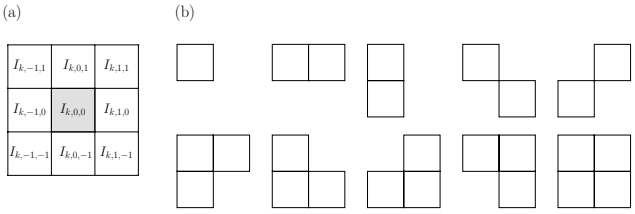

Fig. 2. Eight-pixel neighborhood system with all ten corresponding cliques

where the soft-bit vector $\hat{I}_k = [\hat{i}_{0,k}, \hat{i}_{1,k}, \ldots, \hat{i}_{M-1,k}]$ consists of the individual soft-bits $\hat{i}_{\ell,k} \in \mathbb{R}$ received at the output of the channel. By applying the Bayes theorem we obtain

$$P(I_k = \lambda \,|\, \hat{I}_k, \mathcal{N}_{\hat{I}_k}) = C_k \cdot p(\hat{I}_k \,|\, I_k = \lambda) \cdot P(I_k = \lambda \,|\, \mathcal{N}_{\hat{I}_k}) \quad (6)$$

with the normalization constant C_k. In (6) the term $p(\hat{I}_k \,|\, I_k = \lambda)$ denotes soft-information from the output of the AWGN channel according to

$$p(\hat{I}_k \,|\, I_k = \lambda) = \prod_{\ell=0}^{M-1} p(\hat{i}_{\ell,k} \,|\, i_{\ell,k}), \quad (7)$$

where the conditional p.d.f. $p(\hat{i}_{\ell,k} \,|\, i_{\ell,k})$ for the ℓ-th bit $i_{\ell,k}$ of the index I_k is given in (1) when v_m is replaced with $i_{\ell,k}$. The term $P(I_k = \lambda \,|\, \mathcal{N}_{\tilde{I}_k})$ corresponds to the conditional probability from (3) where the original source indices $I_{k,q,j}$, for the neighborhood are replaced by the estimates $\tilde{I}_{k,q,j}$.

Like in classical Bayesian MRF-based image restoration [6] we use an iterative decoding approach where (6) is applied multiple times until convergence is achieved. The procedure is as follows:

1. Obtain initial estimates $\tilde{I}_k^{(0)}$ for the received 1-D scanned subband image indices by performing a ML decoding from the received soft-bit sequence $\hat{\boldsymbol{I}}$ at the channel output. Set $r \leftarrow 0$.
2. Apply (6) in order to determine the APPs $P(I_k = \lambda \,|\, \hat{I}_k, \mathcal{N}_{\tilde{I}_k^{(r)}})$.
3. Obtain a new estimate $\tilde{I}_k^{(r+1)}$ via a maximum a posteriori (MAP) estimation according to

$$\tilde{I}_k^{(r+1)} = \arg\ \max_{\lambda} P(I_k = \lambda \,|\, \hat{I}_k, \mathcal{N}_{\tilde{I}_k^{(r)}}).$$

4. Set $r \leftarrow r+1$ and go to step 2 as long as the estimates $\tilde{I}_k^{(r)}$ change between iterations.

The resulting APPs $P(I_k = \lambda \,|\, \hat{I}_k, \mathcal{N}_{\tilde{I}_k^{(r)}})$ at the output of the final iteration may be interpreted as approximations of the APPs $P(I_k = \lambda \,|\, \hat{I}_k, \mathcal{N}_{\hat{I}_k})$ conditioned on all received soft-bit vectors $\hat{I}_{k,q,j}$ in the local neighborhood of $\hat{I}_k$.

The calculated APPs can then be used for a mean-squares (MS) estimation, which corresponds to an SNR maximization, according to

$$\hat{U}_k = \sum_{\lambda=0}^{2^M-1} U_q(\lambda) \cdot P(I_k = \lambda \,|\, \hat{I}_k, \mathcal{N}_{\hat{I}_k}). \quad (8)$$

4. ITERATIVE SOURCE-CHANNEL DECODING

An error protection carried out by only using the residual spatial source redundancy may not be enough in many transmission situations. Therefore, we assume that the output of the source encoder is protected by a systematic channel code, as it is depicted in Fig. 1. Note that this scheme is highly similar to a serially concatenated channel code [8], which leads to the iterative decoding scheme depicted in Fig. 3. Herein, the outer constituent channel decoder is replaced by the MRF-based source decoder presented in Section 3.

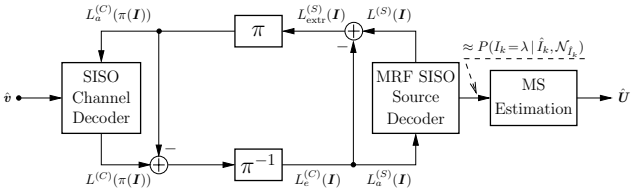

Fig. 3. Iterative source-channel decoder

At the beginning of the first iteration, the SISO channel decoder issues APPs $P(i'_{\ell,k}\,|\,\hat{\boldsymbol{v}})$ for the information bits $i'_{\ell,k}$ of the bit-interleaved source index sequence $\pi(\boldsymbol{I})$. These APPs are used to calculate the corresponding conditional L-values $L^{(C)}(i'_{\ell,k}) = L_c\,\hat{i}'_{\ell,k} + L_a^{(C)}(i'_{\ell,k}) + L_{\text{extr}}^{(C)}(i'_{\ell,k})$ for $\ell = 0,\ldots,M-1,\ k = 0,\ldots,N-1$. The term $L_c\,\hat{i}'_{\ell,k}$ is defined analog to (2) for the interleaved index bit $i'_{\ell,k}$. $L_a^{(C)}(i'_{\ell,k})$ denotes the a priori information for the index bit $i'_{\ell,k}$, and $L_{\text{extr}}^{(C)}(i'_{\ell,k})$ refers to the extrinsic information [10]. After subtraction of the a priori term and after deinterleaving we obtain the L-values $L_{\text{e}}^{(C)}(i_{\ell,k}) = L_c\,\hat{i}_{\ell,k} + L_{\text{extr}}^{(C)}(i_{\ell,k})$, which are used as a priori information $L_a^{(S)}(i_{\ell,k})$ for the SISO source decoder. In the following, we assume that all information bits are uncorrelated. Then, the corresponding index-based probabilities for the a priori L-values $L_a^{(S)}(i_{\ell,k})$ can be obtained by bitwise multiplication of the probabilities for the index bits $i_{\ell,k} = \lambda_\ell$. By inserting this a priori knowledge into (6) we obtain modified APPs according to

$$P'(I_k=\lambda\,|\,\hat{I}_k,\mathcal{N}_{\hat{I}_k}) = C'_k \cdot P(I_k=\lambda\,|\,\mathcal{N}_{\hat{I}_k}) \cdot \prod_{\ell=0}^{M-1} p(\hat{i}_{\ell,k}\,|\,i_{\ell,k}=\lambda_\ell)\,P_{\text{extr}}^{(C)}(i_{\ell,k}=\lambda_\ell\,|\,\hat{\boldsymbol{v}}) \quad (9)$$

where C'_k is a normalizing constant. The initial estimates $\tilde{I}_k^{(0)}$ for the iterative MRF-based source decoding procedure from Section 3 can be directly obtained by using the L-values $L^{(C)}(i_{\ell,k})$. After the iterations have been performed, the output of the SISO source decoder yields the index-based modified APPs $P'(I_k=\lambda\,|\,\hat{I}_k,\mathcal{N}_{\hat{I}_k})$ and the corresponding bit-based L-values $L^{(S)}(i_{\ell,k})$, respectively. By subtracting the source a priori information $L_a^{(S)}(i_{\ell,k})$ from $L^{(S)}(i_{\ell,k})$ we finally obtain the extrinsic information $L_{\text{extr}}^{(S)}(i_{\ell,k})$, which is used as a priori information for subsequent channel decoding.

The convergence behavior of the MRF-based iterative source-channel decoding scheme can be visualized with EXIT charts [11], which show the input-output characteristics of the constituent decoders in terms of mutual information $I(\cdot\,;\cdot)$ between L-values and the index sequence $\boldsymbol{I}$. Given the mutual informations (cmp. Fig. 3)

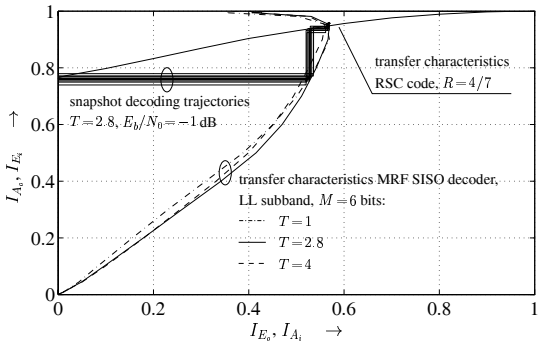

Fig. 4. EXIT chart for the LL subband of the "Goldhill" image ($E_b/N_0 = -1$ dB)

$$I_{E_i} := I(L_e^{(C)}(\pi(\boldsymbol{I}));\pi(\boldsymbol{I})),\quad I_{A_i} := I(L_a^{(C)}(\pi(\boldsymbol{I}));\pi(\boldsymbol{I})),$$
$$I_{E_o} := I(L_{\text{extr}}^{(S)}(\boldsymbol{I});\boldsymbol{I}),\qquad\qquad I_{A_o} := I(L_a^{(S)}(\boldsymbol{I});\boldsymbol{I}),$$

the transfer characteristics T_i of the (inner) channel decoder and T_o of the (outer) MRF SISO decoder are defined as $I_{E_i} = T_i(I_{A_i}, E_b/N_0)$ and $I_{E_o} = T_o(I_{A_o})$, respectively. By plotting both mappings T_i and T_o into one diagram we obtain an EXIT chart, where an example for the LL subband of the "Goldhill" image quantized with $M=6$ bits, a rate $R=4/7$ recursive systematic convolutional (RSC) code, and an $E_b/N_0 = -1$ dB is depicted in Fig. 4. The temperature parameters for the MRF SISO decoder are chosen as $T = 1$, $T = 2.8$, and $T = 4$. We can see from Fig. 4 that for $T = 2.8$ we obtain the highest extrinsic output for almost all values of I_{A_o}. Furthermore, it can be observed that for an increasing mutual information I_{A_o} with $I_{A_o} > 0.9$ the transfer characteristic for the MRF SISO decoder actually leads to a decreasing value of I_{E_o}. This is due to the fact that the MRF model imposes statistical relations on the elements of a local image pixel neighborhood (see (3)). If the channel decoder delivers bits with high reliability, which corresponds to already good initial estimates $\tilde{I}_k^{(0)}$, the imposed statistical dependencies may not hold true for every spatial position within a specific subband image, leading to a quality degradation for the estimates $\tilde{I}_k^{(\ell)}$, $\ell > 0$. In order to illustrate the iterative decoding process Fig. 4 also displays snapshot decoding trajectories, where we can observe that after four iterations convergence is obtained.

5. SIMULATION RESULTS

An experimental image transmission system is derived by applying the transmission model from Fig. 1 to every subband of an L-level wavelet octave filter bank and using the results from above. After optimal scalar quantization the resulting bitstream in each subband is bit-interleaved using a random interleaver and channel encoded with a terminated memory-4 recursive systematic convolutional (RSC) code derived from a nonrecursive RCPC code [12]. Source- and channel coding rates are jointly allocated using the approach from [7]. We assume that sensitive side information, such as the DC content, quantizer stepsizes, and rate allocations, are protected by a sufficiently strong channel code, such that error-free transmission is possible.

The experimental image transmission system is applied to the 512×512 pixel "Goldhill" test image for $L=3$ and a target bit rate of $R_T = 0.37$ bits per pixel (bpp) including channel coding and all

side information. This approach is denoted with "MRF JSCD" in the simulations. The further MRF parameters are $\delta = 0.7$, $T = 2.8$ for the LL subband (cmp. Fig, 4), and $T = 4$ for all other subbands, respectively. Furthermore, we allow a maximum of four iterations in the MRF source decoder. We compare the performance of the presented approach with the method from [7] ("2-D JSCD") which employs a similar iterative source-channel decoding setup, but a different source model. In this model, horizontal and vertical correlations are regarded as separate Markov sources, where the transition probabilities corresponding to these Markov processes are obtained from a large training set and are stored at the decoder. Besides, plain MRF-based source decoding ("MRF SD") without additional protection by channel codes is considered. For all approaches, a mean-squares estimation is employed.

Fig. 5 shows the simulation results for the above-mentioned methods where the peak-SNR (PSNR) values of the reconstructed images versus the channel parameter E_b/N_0 averaged over 100 simulated transmissions are displayed. Especially for low channel SNR the "MRF JSCD" technique outperforms the "2-D JSCD" approach by approximately 1-2 dB in PSNR, where we have observed similar gains also for other images. This performance gain may be due to the fact that the MRF source decoding itself is performed iteratively, such that the channel decoder can be provided with more reliable L-values for the next iteration. For channels with an $E_b/N_0 > 1$ dB both approaches have approximately the same performance. In our simulations we observed that the "MRF JSCD" approach approximately has the same complexity as the the "2-D JSCD" approach. However, the storage complexity is significantly reduced for the proposed MRF-based JSCD approach since there is no need to store source a priori information. An example

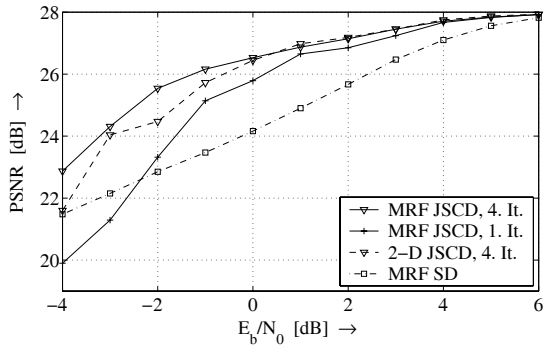

Fig. 5. Results for the "Goldhill" image ($R_T = 0.37$ bpp, $L = 3$)

of the good reconstruction quality for a highly corrupted channel is displayed in Fig. 6.

6. CONCLUSIONS

By using the implicit two-dimensional residual source redundancy for error protection in conjunction with channel coding, an iterative decoding scheme is derived in a similar way as for serially concatenated channel codes: the difference is that a soft-input APP source decoder replaces the outer constituent channel decoder. The source signals are modeled using Markov random fields, and due to the Markov-Gibbs correspondence, the computation of a priori densities can be made very resource-efficient. We have shown that this source-channel decoding technique can be used for robust image transmission over highly distorted AWGN channels. The simulation results show that clear-channel quality is already achieved for an E_b/N_0 of as little as 4 dB.

Fig. 6. Reconstructed image for $E_b/N_0 = -1$ dB (bit error rate 10.4 %), PSNR 26.23 dB ($R_T = 0.37$ bpp, $L = 3$, MRF JSCD, four iterations).

7. REFERENCES

[1] P. G. Sherwood and K. Zeger, "Error protection for progressive image transmission over memoryless and fading channels," *IEEE Trans. on Comm.*, vol. 46, no. 12, pp. 1555–1559, 1998.

[2] V. Chande and N. Farvardin, "Joint source-channel coding for progressive transmission of embedded source coders," in *Proc. IEEE Data Compression Conference*, Snowbird, UT, USA, Mar. 1999, pp. 52–61.

[3] H. H. Otu and K. Sayood, "A joint source/channel coder with block constraints," *IEEE Trans. on Comm.*, vol. 47, no. 22, pp. 1615–1618, Nov. 1999.

[4] M. Park and D. J. Miller, "Improved image decoding over noisy channels using minimum mean-squared estimation and a Markov mesh," *IEEE Trans. on Image Proc.*, vol. 8, no. 6, pp. 863–867, June 1999.

[5] M. Adrat, R. Haenel, and P. Vary, "On joint source-channel decoding for correlated sources," in *Proc. IEEE Int. Conf. Acoust., Speech, Signal Processing*, Orlando, FL, USA, May 2002, pp. 2505–2508.

[6] S. Geman and D. Geman, "Stochastic relaxation, Gibbs distribution, and the Bayesian restoration of images," *IEEE Trans. on Pattern Analysis and Machine Intelligence*, vol. PAMI-6, no. 6, pp. 721–741, Nov. 1984.

[7] J. Kliewer and N. Goertz, "Iterative source-channel decoding for robust image transmission," in *Proc. IEEE Int. Conf. Acoust., Speech, Signal Processing*, Orlando, FL, USA, May 2002, pp. 2173–2176.

[8] S. Benedetto, D. Divsalar, G. Montorsi, and F. Pollara, "Serial concatenation of interleaved codes: Performance analysis, design, and iterative decoding," *IEEE Trans. on Inf. Theory*, vol. 44, no. 3, pp. 909–926, May 1998.

[9] C. A. Bouman and K. Sauer, "A generalized Gaussian image model for edge-preserving MAP estimation," *IEEE Trans. on Image Processing*, vol. 2, no. 3, pp. 296–310, July 1993.

[10] J. Hagenauer, E. Offer, and L. Papke, "Iterative decoding of binary block and convolutional codes," *IEEE Trans. on Inf. Theory*, vol. 42, no. 2, pp. 429–445, Mar. 1996.

[11] S. ten Brink, "Code characteristic matching for iterative decoding of serially concatenated codes," *Annals of Telecomm.*, vol. 56, no. 7-8, pp. 394–408, July-August 2001.

[12] J. Hagenauer, "Rate-compatible punctured convolutional codes (RCPC codes) and their appplications," *IEEE Trans. on Comm.*, vol. 36, no. 4, pp. 389–400, Apr. 1988.